Effects of Vision Restoration Training on Early Visual Cortex in Patients With Cerebral Blindness Investigated With Functional Magnetic Resonance Imaging

M. Raemaekers, D. P. Bergsma, R. J. A. van Wezel, G. J. van der Wildt and A. V. van den Berg

J Neurophysiol 105:872-882, 2011. First published 15 December 2010; doi:10.1152/jn.00308.2010

J Neurophysiol 105: 872–882, 2011.
First published December 15, 2010; doi:10.1152/jn.00308.2010.

Effects of Vision Restoration Training on Early Visual Cortex in Patients With Cerebral Blindness Investigated With Functional Magnetic Resonance Imaging

M. Raemaekers,[1] D. P. Bergsma,[1] R. J. A. van Wezel,[1,2,3] G. J. van der Wildt,[1] and A. V. van den Berg[1,4]
[1]*Helmholtz Institute and* [2]*Utrecht Institute of Pharmaceutical Sciences, Utrecht University, Utrecht;* [3]*Biomedical Signals and Systems, University of Twente, Enschede; and* [4]*Department of Medical Physics and Biophysics, Radboud University Medical Center, Nijmegen, The Netherlands*

Submitted 1 April 2010; accepted in final form 13 December 2010

Raemaekers M, Bergsma DP, van Wezel RJA, van der Wildt GJ, van den Berg AV. Effects of vision restoration training on early visual cortex in patients with cerebral blindness investigated with functional magnetic resonance imaging. *J Neurophysiol* 105: 872–882, 2011. First published December 15, 2010; doi:10.1152/jn.00308.2010. Cerebral blindness is a loss of vision as a result of postchiasmatic damage to the visual pathways. Parts of the lost visual field can be restored through training. However, the neuronal mechanisms through which training effects occur are still unclear. We therefore assessed training-induced changes in brain function in eight patients with cerebral blindness. Visual fields were measured with perimetry and retinotopic maps were acquired with functional magnetic resonance imaging (fMRI) before and after vision restoration training. We assessed differences in hemodynamic responses between sessions that represented changes in amplitudes of neural responses and changes in receptive field locations and sizes. Perimetry results showed highly varied visual field recovery with shifts of the central visual field border ranging between 1 and 7°. fMRI results showed that, although retinotopic maps were mostly stable over sessions, there was a small shift of receptive field locations toward a higher eccentricity after training in addition to increases in receptive field sizes. In patients with bilateral brain activation, these effects were stronger in the affected than in the intact hemisphere. Changes in receptive field size and location could account for limited visual field recovery (±1°), although it could not account for the large increases in visual field size that were observed in some patients. Furthermore, the retinotopic maps strongly matched perimetry measurements before training. These results are taken to indicate that local visual field enlargements are caused by receptive field changes in early visual cortex, whereas large-scale improvement cannot be explained by this mechanism.

INTRODUCTION

Cerebral blindness refers to a condition in which the patient suffers from visual field defects as a consequence of postchiasmatic damage to the visual pathways. This condition is in most cases the result of stroke, causing an estimated number between 90,000 and 100,000 of new cases of cerebral blindness each year in the United States and Europe alone (Sahraie 2007). In the last 15 yr, an increasing number of studies have shown that the effects of brain injury to the visual pathways can be reversed through training to some extent also in patients with older lesions (>2 yr) and stable deficits (Bergsma and Van der Wildt 2008, 2010; Julkunen et al. 2003; Kasten et al. 1998a,b, 2000, 2006; Mueller et al. 2007; Poggel et al. 2001; Schmielau and Wong Jr 2007; Van der Wildt and Bergsma 1997; however, also see Reinhard et al. 2005). During training, subjects are requested to repeatedly fixate their gaze on a central point and detect stimuli at the border zone between the functioning and impaired portion of the visual field, which results in gradual enlargement of the visual field (Bergsma and Van der Wildt 2010).

The neuronal mechanisms through which this restoration of vision occurs are still not fully understood. As a result, the assessment of gain through training is mostly based on first person reports. Therefore we want to address visual field recovery with more objective measures. Recent imaging studies have shed light on some possible neuronal mechanisms for recovery. Henriksson et al. (2007) observed that after extensive training, the intact hemisphere processed the information from both hemifields in a subject with homonymous hemianopia, which implies that voxels in the intact hemisphere gained a second receptive field in the other hemifield, suggesting the potential for massive reorganization. The notion that therapy can induce structural changes is further supported by a functional magnetic resonance imaging (fMRI) study that found indirect evidence for changing receptive field properties in patients with macular degeneration (Schumacher et al. 2008). On the other hand, Ho et al. (2009) measured the presence of brain activation that represented a portion of the visual field that was damaged according to perimetry. Such residual capacity could be a possible target for vision restoration training. However, considering the variation in brain damage and the outcome of training of individual patients, it is imperative that the neuronal mechanisms that play a role in training are not only assessed in case studies.

In the current study we investigated the properties of early visual cortex (V1, V2, and V3) before and after vision restoration training by measuring changes in blood oxygenation level dependent (BOLD) responses during retinotopic mapping stimuli in a heterogeneous experimental group, considering size and nature of the lesion and the size of visual field loss. We assessed between session differences in amplitude, onset time, and width (dispersion) of BOLD responses during the mapping stimuli in V1, V2, and V3. These differences in BOLD responses respectively reflected changes in the strength of the visually evoked responses, changes in the location of the receptive fields of voxels, and changes in the receptive field

Address for reprint requests and other correspondence: M. Raemaekers, Helmholtz Institute, Utrecht University, Limalaan 30, 3584 CL Utrecht, The Netherlands (E-mail: m.raemaekers-2@umcutrecht.nl).

sizes of voxels. In addition we assessed whether there were changes in amplitudes of a second BOLD response per cycle, to assess whether voxels gained a second receptive field as a result of training, which would be predicted based on the results of Henriksson and colleagues (2007). Our data indicated that training induced small shifts of receptive field locations toward the eccentricity, in addition to increases in receptive field size, which could explain small visual field recovery.

METHODS

Subjects

Eight patients with one-sided homonymous visual field defects volunteered for participation via a website. All subjects gave informed consent for participation, approved by the local ethics committees of the University Medical Center in accordance with the Declaration of Helsinki of the World Medical Association. When necessary, subjects wore MR-compatible glasses. The minimum time postlesion at the onset of training was 6 mo to avoid confounding of training effects by natural recovery (Zhang et al. 2006). As an additional check, all patients (except patient 6) were measured twice before commencing the training and no patient showed any change in the size of the visual field defect. A summary of the subject data is shown in Table 1. Locations of the lesion for the eight patients were the following.

PATIENT 1. The medial part of the right occipital lobe, including the area around the calcarine sulcus, and the ventral part of the posterior temporal cortex.

PATIENT 2. The dorsoanterior part of the area around the left calcarine sulcus.

PATIENT 3. The left lateral geniculate nucleus. The occipital lobe was unaffected.

PATIENT 4. The dorsoanterior part of the area around the right calcarine sulcus.

PATIENT 5. The medial part of the left occipital lobe, including the inferior part of the area around the calcarine sulcus, and the posterior part of the medial temporal lobe.

PATIENT 6. The dorsolateral part of the right occipital lobe, the inferior parietal lobe, and the dorsal part of the posterior temporal cortex. The area around the calcarine sulcus was unaffected.

PATIENT 7. The ventroanterior part of the area around the left calcarine sulcus.

PATIENT 8. Small lesion affecting the lateral part of the area around the right calcarine sulcus.

TABLE 1. *Profile of subjects*

Subject	Age, yr	Sex	Type of Stroke	OTTPL, mo	Pre-ACFS	Post-ACFS
1	54	Male	Ischemic	40	<1°	1°
2	61	Female	Ischemic	8	6°	12°
3	26	Male	Hemorrhagic	72	1°	2°
4	53	Male	Ischemic	9	6°	12°
5	69	Male	Ischemic	6	2°	9°
6	66	Male	Hemorrhagic	106	2°	9°
7	46	Female	Ischemic	12	<1°	4°
8	73	Male	Ischemic	13	5°	9°

OTTPL, onset training time postlesion; ACFS, average central field sparing pre- or posttraining.

MRI scans providing details on the location and the extent of the lesion for each patient are shown in Fig. 1. We did not include patients that displayed fixation problems during the intake procedure.

Training and perimetry measurements

Training was performed on a manual Goldmann perimeter. Subjects were trained monocularly for both eyes consecutively with repeated trials of stimulus detection threshold measurements. Background luminance was 31.5 apostilb (asb; $\approx$10 cd/m^2). Luminance of the white, circular stimulus (Goldmann IV, diameter: 1°) was set at 12.5 asb (IV-1a $\approx$ 4 cd/m^2) and was increased stepwise with a 0.1 log unit change $\leq$1,000 asb (IV-4e $\approx$ 318 cd/m^2). Subjects responded after stimulus detection during central fixation. Subjects were presented with a wide-ranged set of stimuli on fixed locations in the damaged portion of the visual field. During training, fixation was monitored visually so that small changes in eye position could be detected. However, when a subject starts a session with a parafoveal fixation, it can be detected only if the deviation from the fixation point is large enough. Therefore in addition, the blind spot is probed on several occasions during each training session to check for parafoveal fixation. During perimetry, gaze direction was continuously monitored with an eye tracker (EyeLink II). Using the eye tracker data, trials with inadequate fixation could be discarded, so that perimetry was based on trials with adequate fixation alone. The method is described in more detail in Bergsma and Van der Wildt (2008). Subjects were trained under constant supervision during a period of 10 wk. There were four sessions of 1 h each week, making a total of 40 training hours per subject.

Scanning protocol

Subjects participated in two scanning sessions with an interval of 10 wk. Scanning was performed on a Philips Achieva 3T scanner (Philips Medical Systems, Best, The Netherlands) with a Quasar dual-gradient set. For functional images, a SENSE (sensitivity encoding) implementation of a navigated 3D-PRESTO (three-dimensional principle of echo shifting with a train of observations) pulse sequence was used (Golay et al. 2000; Neggers et al. 2008). PRESTO sequences allow very short acquisition times by already applying the next excitation before signal readout using a technique called echo shifting. Slices were acquired in the coronal orientation. The acquisition parameters were: repetition time (TR) = 30 ms (time between two subsequent radiofrequency pulses); effective time to echo (TE) = 43.87 ms; field of view (FOV: inferior–superior, right–left, anterior–posterior) = 200 $\times$ 160 $\times$ 65 mm; flip angle = 10°; matrix: 80 $\times$ 64 $\times$ 26 slices; voxel size: 2.5 mm isotropic; 8-channel head coil; SENSE factors = 2.0 (left–right) and 1.8 (anterior–posterior). A new volume was acquired every 540 ms and encompassed the posterior 65 mm of the brain. A T1-weighted structural image of the whole brain (voxel resolution = 0.875 $\times$ 0.875 $\times$ 1.00 mm; FOV = 168 $\times$ 224 $\times$ 160 mm) was acquired in transversal orientation at the end of the functional series on both scanning days. A total of 3,704 images were acquired in four series during each session, with a mean duration of 500 s per series.

Stimuli

The procedures and stimuli for session 1 and session 2 were identical. For task presentation we used a desktop PC, a projection screen, and a video-projector system. The start of each series of stimuli was triggered by the scanner. During all stimuli, there was a red central fixation dot (radius of 0.1° visual angle) that was surrounded by a circular aperture (radius of 0.5° visual angle). Subjects were requested to maintain fixation on the fixation dot regardless of the presented stimuli. For eccentricity mapping, we used a contracting ring with a maximum eccentricity of 7.5°

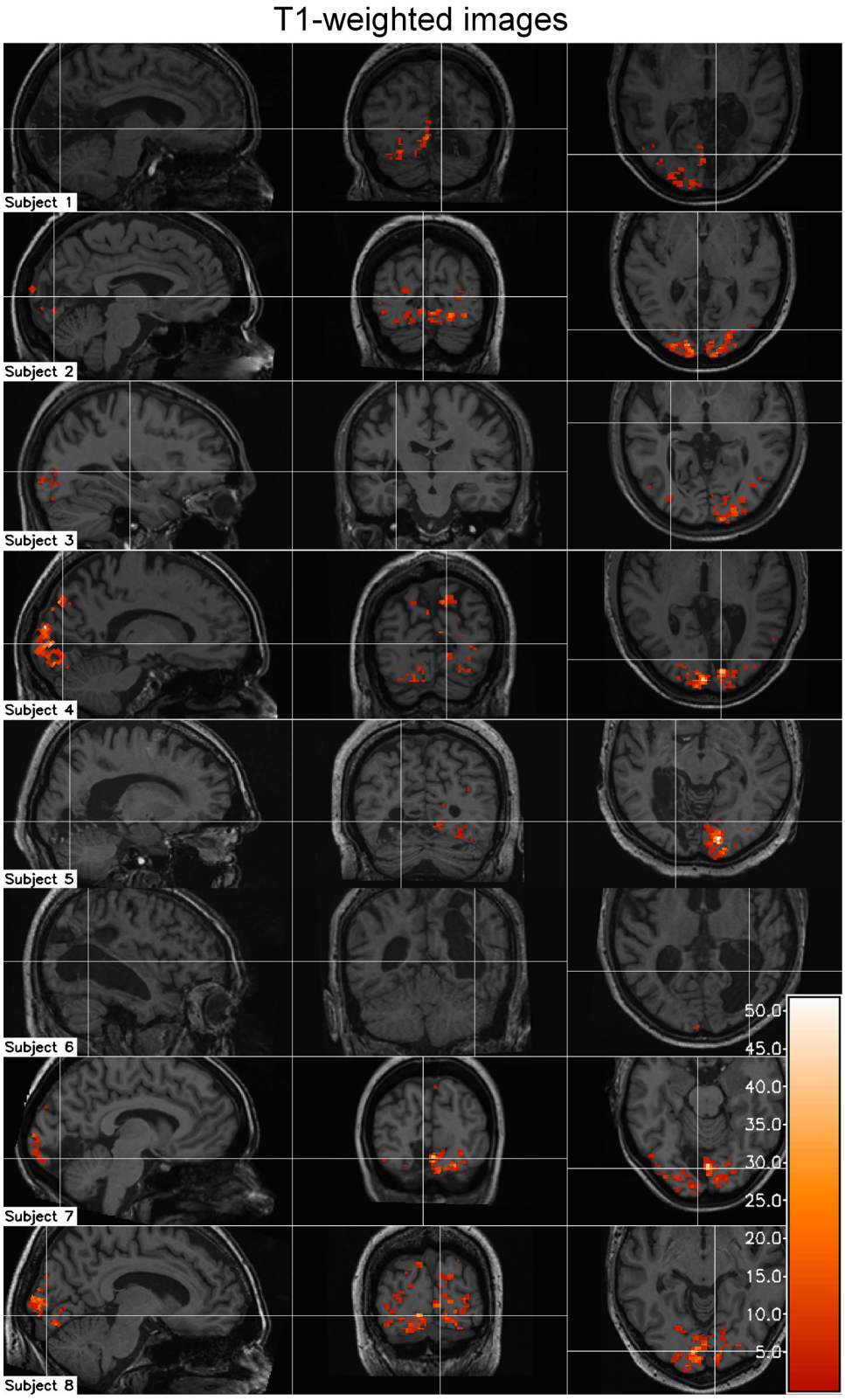

FIG. 1. T1-weighted images of the patients. Slices are chosen for each patient individually to optimally show the location and extent of the lesion. Scans are positioned in Talairach orientation and are displayed according to the neurological convention. The white cross is centered on the lesion and indicates the x, y, and z locations of the shown slices. Superimposed in red-yellow are the voxels that had a significant blood oxygenation level dependent (BOLD) response during polar angle mapping and during eccentricity mapping before and after training. The red-yellow intensity represents the mean f-value for polar angle mapping and eccentricity mapping before and after training.

visual angle. After the ring was fully contracted (0.5° eccentricity), it returned to its maximum eccentricity. The width of the ring changed with eccentricity. There were two runs of eccentricity mapping, each containing eight stimulus cycles of 60 s, with a total duration of 960 s (1,778 functional images). For polar angle mapping, we used a rotating wedge (18° circular angle) that extended to a maximum eccentricity of 7.5° visual angle. There were two runs of polar angle mapping, each containing stimulus 26 cycles of 20 s, with a total duration of 1,040 s (1,926 functional images). Both the rotating wedge and the expanding ring contained a checkerboard pattern with green and red squares that reversed color every 125 ms. There were no resting periods during the stimulus presentation. The start of each stimulus cycle of the wedge and the ring

was logged to a file. Eye movements were not recorded during the scanning sessions.

Statistical analysis

All spatial preprocessing steps were done using SPM5 (//www.fil.ion.ucl.ac.uk/spm/). The functional images of both scanning sessions were realigned in a two-pass procedure to the mean functional image and subsequently resliced. No smoothing was applied. Further analysis steps were performed in combination with custom routines in IDL (Research Systems, Boulder, CO) and were done separately for each scanning session and for polar angle and eccentricity mapping. For removing low-frequency noise from the data, a design matrix was created containing the mean of each image and cosine functions forming a high-pass filter with a cutoff at twice the duration of a stimulus cycle (26 cosine functions per series of polar angle mapping and 8 cosine functions per series of eccentricity mapping). The mean of each factor was removed from the design matrix and a model was estimated for each voxel using a general linear model. The estimated model, with the exception of the intercept, was subtracted from the data. The filtered data were subsequently rescaled to percentage signal change relative to the mean signal.

Two design matrices, containing 20 finite impulse response (FIR) functions each, were created for the polar angle mapping and for the eccentricity mapping using SPM5. The window length used was the duration of one stimulus cycle. The coefficient estimates for the impulse functions form the average BOLD response during a stimulus cycle of either polar angle mapping of eccentricity mapping (both interpolated to 20 time points). The design matrices were separately applied to the functional data of session 1, to the functional data of session 2, and to the signal difference between the two sessions. This resulted in 2 (polar angle and eccentricity) $\times$ 3 (session 1, session 2, and the difference between the sessions) $\times$ 20 (number of impulse functions) volumes with regressor coefficient estimates and 2 $\times$ 3 volumes with f-values for the FIR models.

The mean BOLD responses per stimulus cycle (i.e., the maps containing the regressor coefficients of the FIR model) were used for further analysis. The purpose was to determine for each voxel and each session: *1*) the amplitude of the BOLD response, *2*) the timing of the BOLD response (i.e., a difference in receptive field location), and *3*) the width of the BOLD response (i.e., the receptive field size). To reduce processing time, this analysis was performed on the mean BOLD responses for each stimulus cycle, instead of the complete time series. A matrix with 400 (20 $\times$ 20) curves was created that represented BOLD responses with different onsets (20 polar angle or eccentricity steps) and different dispersions (20 steps). These curves were generated by creating blocked neural responses with different onset times and durations and convolving the blocked neural responses with a BOLD response. All curves were scaled between 0 and 1. A schematic representation of the matrix with the curves is presented in Fig. 2. Each curve was fitted to the BOLD responses in each voxel of session 1 and session 2 using a linear regression. The estimated dispersion and polar angle/eccentricity for each session were selected by the factor with the highest correlation. The estimated regressor coefficient of the curve with the highest correlation represented the amplitude. Thus for each session, a model of the BOLD response was created that demonstrated a best fit with the data considering amplitude, onset, and dispersion. Subsequently, it was estimated for each voxel before and after training whether the mean response it demonstrated was significantly BOLD-like. This was done by calculating the product of the f-value of the FIR model for the separate sessions and the R^2 of the fit of the model of the BOLD response on the mean response. Only voxels that showed a significant BOLD-like response before and after training ($P < 0.05$, Bonferroni corrected) were considered for analysis of changes in amplitude, lag, and dispersion. For information on the number of voxels that met this criterion and the number of voxels that were discarded, see Supplemental Material S1.[1] An additional analysis was performed to detect the presence of a second peak representing a second receptive field. Therefore the fitting process was repeated on the residual responses (i.e., the mean response after regressing out the curve with the highest fit).

To estimate whether between session differences in amplitude, lag, and dispersion were significant, we calculated the amount of variance of the responses of the second session after:

1 *Subtraction of the model of session 1.*

2 *Subtraction of the model of session 1, but with the estimated amplitude of session 2.*

3 *Subtraction of the model of session 1, but with the estimated amplitude and onset of session 2.*

4 *The model of session 2.*

The reduction in variance with each calculation (1 to 4) is related to changes between sessions in amplitude (1–2), changes in onset (2–3), and changes in dispersion (3–4) of the BOLD response. The reduction in variance with each step was subsequently expressed as a proportion of the total between session variance. An estimate of the corresponding f-value could then be given by the product of this percentage and the f-value of the FIR model for the difference between sessions. This resulted in F-maps for differences in amplitude, onset, and dispersion of the BOLD response. Examples of mean responses during stimulus cycles and the corresponding fitted models are shown in Fig. 3.

Segmentation of retinotopic areas

The T1 images from both sessions were corrected for intensity inhomogeneities using the segmentation utility in SPM5 (Ashburner and Friston 2005) and subsequently registered and averaged. Surface reconstructions were made using the Computerized Anatomical Reconstruction and Editing Tool Kit (CARET; Van Essen et al. 2001). When field maps were sufficiently intact, retinotopic areas V1, V2, and V3 were manually segmented by drawing borders along the reversals in the change of the polar angle representation. An additional segment was drawn manually on the noninflated surface that encompassed the anatomical location of V1, V2, and V3 in both the intact and damaged hemispheres. When the retinotopic maps were too damaged for normal drawing, this segment was drawn based on the assumption of symmetry in functional anatomy between hemispheres. This was the case for patients 1, 3, 5, 6, and 7. An example of a segment is shown in Fig. 4 (for subject 7). Note that no specific statements regarding the location of activation in these areas can be made. The segment was also somewhat dilated to ascertain that it enclosed V1–V3, also in the damaged hemisphere. The resulting segment for each patient is shown in Fig. 1. These segments were used as a search area for visual activation. All surface segments were converted back to volumetric format and used as regions of interest in further analyses.

RESULTS

Perimetry results

All but one patient showed an increase in visual field size following training. The average central field sparing (ACFS) was before and after training can be seen in Table 1. Although most patients benefited from training, the amount of increase varied considerably between patients, but was significant (mean increase in ACFS = 3.94°; SD = 2.75°; Wilcoxon signed-ranks test $Z = 2.38$; $P = 0.017$). Perimetry results for the central 15° part of the visual field (i.e., the part of the visual

[1] The online version of this article contains supplemental data.

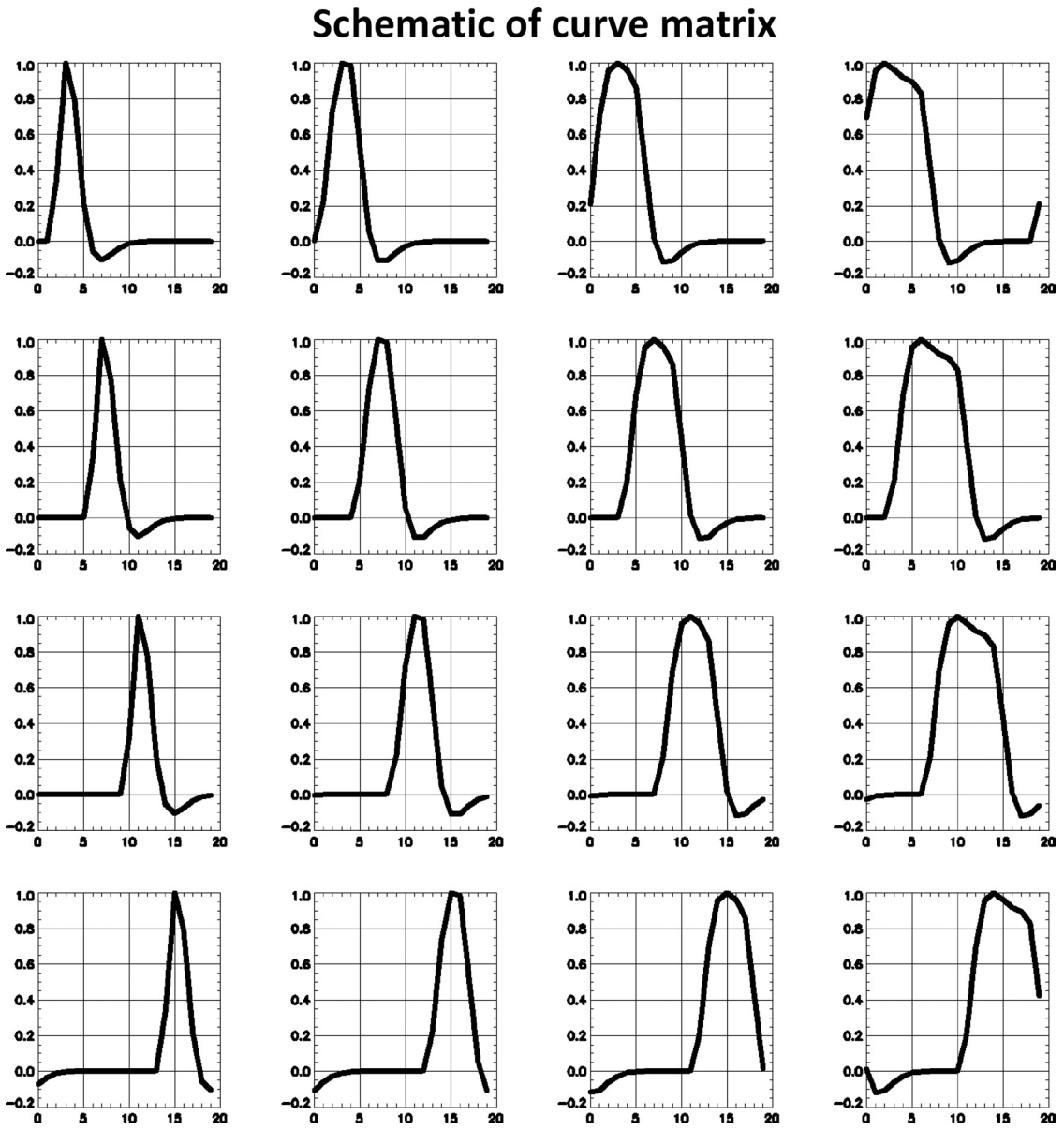

FIG. 2. Schematic of the matrix of curves that were sequentially fitted to the mean responses. Note that the real matrix contained 20 × 20 steps. The dispersion increases over the horizontal axis and the lag increases over the vertical axis.

field that was mapped with fMRI) can also be seen in Fig. 5. No shift in the blind spot was observed in the eight patients. Note that considering the relatively large size of the blind spot, this method may not be sufficient to detect very small deviations from central fixation.

fMRI results

fMRI results were compared with perimetry results by plotting the receptive field locations of individual voxels on the visual fields as measured with perimetry (Fig. 5). Voxels were plotted only when the voxels demonstrated a significant BOLD-like response during both polar angle mapping and eccentricity mapping and both before and after training. This was to ascertain that the amplitude, lag, and dispersion of the voxel could always be adequately determined for both sessions. It is possible that this restriction neglects training-induced changes in voxels that are significantly BOLD-like in only one of the sessions. When this was the case (i.e., the amplitude of the responses differed significantly between sessions and was significantly BOLD-like in only one of the sessions), the receptive field locations corresponding to the significant response were plotted in a separate figure (Supplemental Material S2). In addition, voxels had to be located within the anatomical location of the early visual cortex (as shown in Fig. 1). Note that for patients 1, 3, 5, 6, and 7 the location of early visual cortex within the damaged hemisphere was defined based on the symmetry assumption with the contralateral hemisphere. For these patients, the localization of unclassified voxels (Supplemental Material S2) is thus based on an estimation. When there was a significant difference between sessions in lag, or dispersion, during either polar angle mapping or eccentricity mapping, this is indicated in the plots of Fig. 5 ($P < 0.05$, Bonferroni corrected). When there was no

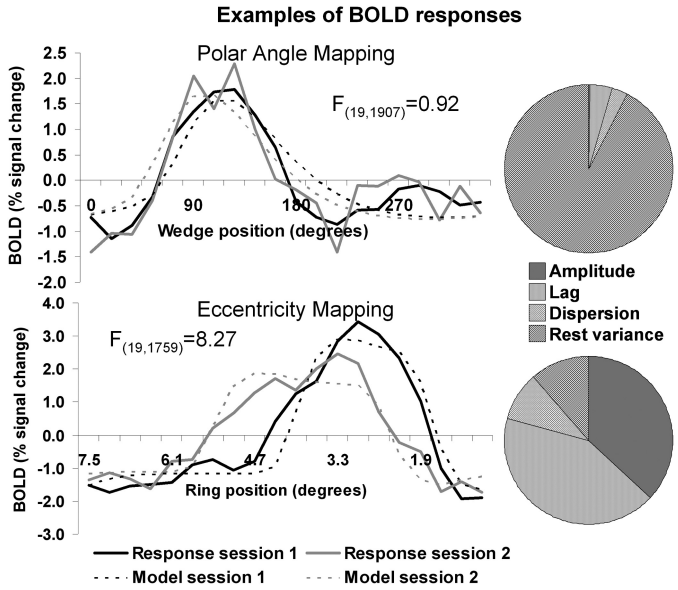

FIG. 3. Example of average BOLD responses as estimated with the finite impulse response (FIR) model in a voxel of patient 2 during polar angle mapping and eccentricity mapping. The amplitude of the BOLD response is relative to the mean signal during the cycle. This voxel had different responses during eccentricity mapping, but not during polar angle mapping. The corresponding models with the best fit considering amplitude, lag, and dispersion are plotted in the same graph with dotted lines. The f-value for the difference in responses between sessions is indicated in the graphs. The circular plots on the right give the estimates of the proportion of the between session variance that is caused by changes in amplitude, lag, and dispersion.

significant difference in lag during polar angle or eccentricity mapping, the mean lags over the two sessions were used for plotting. Visual field locations of voxels separated for V1, V2, and V3 are shown in Supplemental Material S2.

Changes in receptive field locations

Visual inspection of the results revealed that most voxels did not show a significant difference in receptive field location between sessions, indicating no evidence for large-scale reorganization of early visual cortex by training (mean percentage of voxels per subject without a difference = 96.7%; SD = 2.2%). However, in most voxels that did show a change, the receptive field was shifted toward a higher eccentricity (mean percentage of voxels that showed a significant shift toward the eccentricity = 87.6%; SD = 17.4%). The mean shift toward higher eccentricity in all voxels was although very moderate significant over subjects [paired $t_{(7)} = 4.09$; $P = 0.005$; median change = 0.13°] (Fig. 6*A*). In addition, this mean shift was much larger in the affected hemisphere than that in the nonaffected hemisphere in all three subjects (patients 2, 4, and 8) with bilateral visual activation [mean shift in the affected hemisphere = 0.35°; SD = 0.06°; mean shift in the intact hemisphere = 0.10°; SD = 0.07°; paired $t_{(2)} = 12.9$; $P = 0.006$].

Changes in amplitudes and dispersion

A number of voxels showed a change in amplitude of the BOLD response with training, either during polar angle mapping, eccentricity mapping, or both (mean percentage of voxels per subject with a difference in BOLD amplitude = 11.7%; SD = 10.0%). Most of these voxels showed a decrease in activation (mean percentage of voxels with a reduction = 81.0%; SD = 15.5%). The mean reduction over all voxels was not significant [paired $t_{(7)} = -2.13$; $P = 0.071$; median change = −0.37%]. In addition, there was a small proportion of voxels with a difference in dispersion between sessions. These differences in dispersion were observed only during eccentricity mapping (mean percentage of voxels per subject with a difference in BOLD dispersion = 1.2%; SD = 10.0%). Note that the cycle duration was much shorter during polar angle mapping, which may have caused insensitivity for detecting changes in receptive field size through dispersion during polar angle mapping. Most of the voxels showed an increase in dispersion (mean percentage of voxels with an increase = 93.1%; SD = 11.1%). The mean increase of all voxels was significant [paired $t_{(7)} = 2.54$; $P = 0.04$; median change = 392.3] (Fig. 6*C*). This effect was also larger in the affected hemisphere of all three patients with bilateral visual activation [mean increase in the affected hemisphere = 2.0; SD = 0.3; mean shift in the intact hemisphere = 0.1; SD = 1.0; paired $t_{(2)} = 4.54$; $P = 0.045$]. There was no significant correlation between changes in dispersion and amplitudes of the BOLD response ($r = 0.483$; $P = 0.225$). Changes in dispersion or amplitudes of the BOLD response did not correlate with the shift toward a higher eccentricity (correlations were 0.063 and −0.056, respectively; both n.s.).

Comparing fMRI retinotopic maps and perimetry visual field maps

To assess the possibility for the presence of residual capacity, meaning that the regained field was represented before (and after) training, we compared the fMRI to the perimetry results. To estimate whether differences in the density of voxels between the intact, regained, and nonregained visual field were significant, we performed three binomial tests for each subject. Because differences between sessions in receptive field locations of voxels were very small (Fig. 5), we used the mean location of both sessions because this provided a more reliable estimate. These tests compared the density in, respectively: *1*) the intact and regained visual field; *2*) the intact and nonregained visual field; and *3*) the regained and nonregained visual field. Note that for estimation of the probability of a success of a single event (a voxel is located within a particular

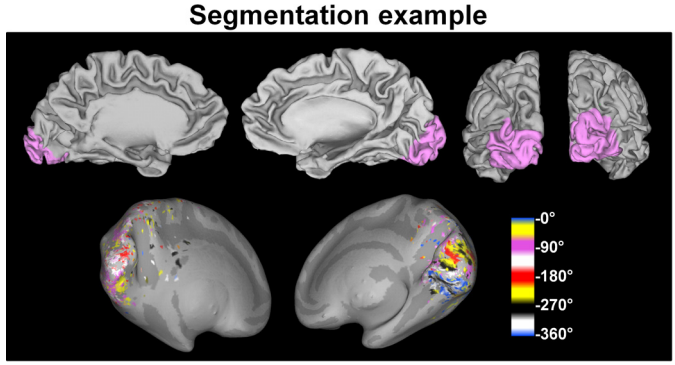

FIG. 4. Illustration of the segmentation for subject 7. The left visual cortex was damaged; therefore an outline for a search area for visual activation was drawn based on the intact hemisphere. Purple shows the segment that was drawn for this subject for the left and right hemispheres.

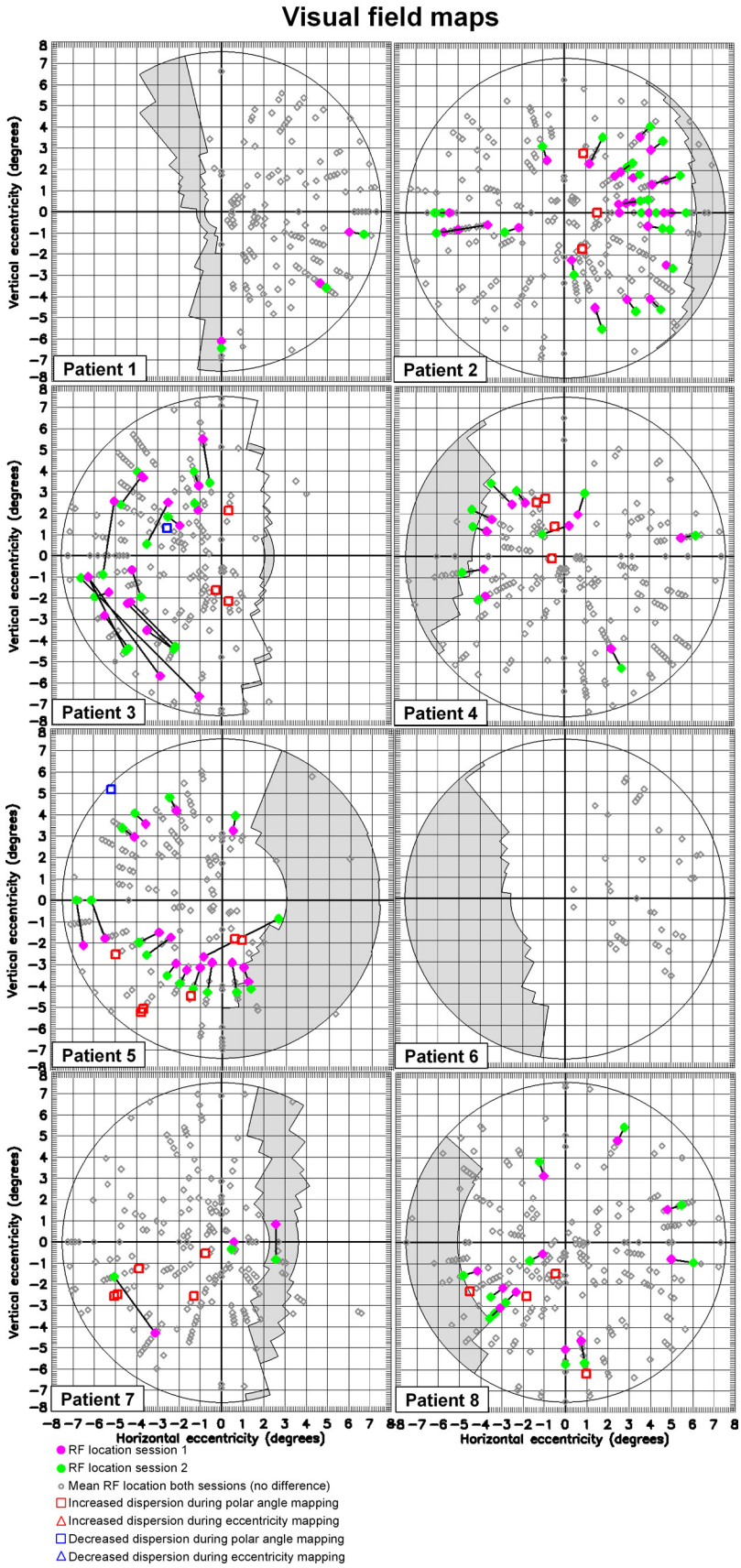

FIG. 5. Visual field maps of the eight patients as measured with perimetry and with fMRI before and after training. Perimetry results are shown in the background by the partial circle in gray and white. The white delineated portion of the circle represents the visual field where stimuli were detected before and after training. In the gray delineated portion, stimuli were only detected after training. The undelineated portion was blind before and after training. Superimposed are visual field locations that were represented by voxels in early visual cortices as measured with fMRI. When a significant difference in lag was present, the represented location of the first session in shown in purple and the location of the second session is shown in green.

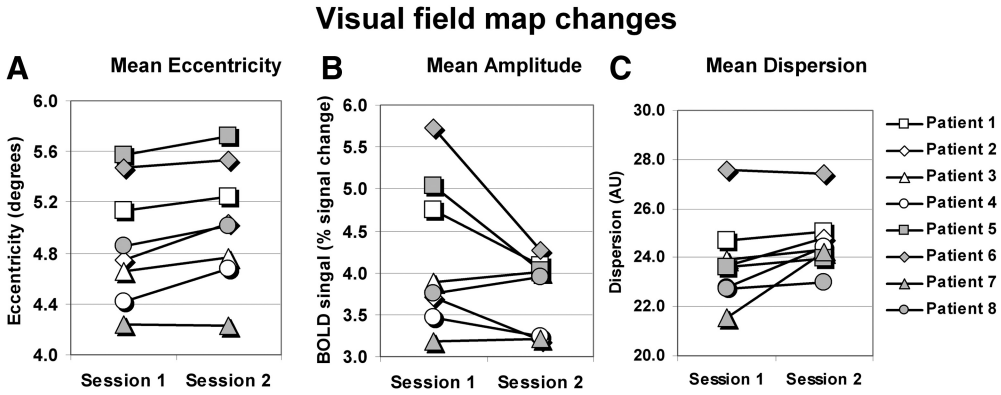

FIG. 6. For all subjects the mean change over all voxels in visual field maps considering. *A*: eccentricity of receptive field locations. *B*: amplitude of BOLD responses. *C*: dispersion of BOLD responses. The used stimuli did not allow for estimation of absolute receptive field sizes and are therefore expressed in arbitrary units.

portion of the visual field), we used the percentage of polar angle/eccentricity combinations (20 polar angle steps × 20 eccentricity steps) that were located within a particular portion of the visual field. There was a clear difference between the intact and the regained field in nearly all subjects (Table 2). The number of voxels representing the regained visual field was thus very low compared with that of the intact visual field. Note that in subjects where the difference was least significant, the size of the recovered visual field (in the scanner) tended to be smaller (Spearman's rho = 0.62; $P = 0.051$, one-sided). As in most patients the visual field recovery extended beyond the size of the visual field that we could measure from within the MRI scanner, we could not make reliable comparisons with the nonregained visual field.

Second responses during cycles

We compared the mean amplitudes of the second fitted response between sessions for polar angle mapping and eccentricity mapping. A second response during a cycle of a mapping stimulus indicates the presence of a second receptive field within a voxel, as would be predicted on the basis of previous research (Henriksson et al. 2007). There was a small and nonsignificant reduction in the amplitude of BOLD responses during both polar angle mapping and eccentricity mapping after training [for eccentricity mapping: mean amplitude before = 1.66; mean amplitude after = 1.51; $t_{(7)} = -1.51$; $P = 0.18$; for polar angle mapping; mean amplitude before = 0.61; mean amplitude after = 0.57; $t_{(7)} = 0.90$; $P = 0.397$]. Note that the duration of a stimulus cycle during polar angle mapping was most likely too short for detecting secondary responses, which is reflected by the lower amplitude estimates of the second response.

TABLE 2. *P values corresponding to the binomial tests that contrasted the number of vowels representing the different portions of the visual field*

Subject	Intact vs. Regained	Intact vs. Nonregained	Regained vs. Nonregained
Patient 1	0.000	0.000	0.306
Patient 2	0.362	—	—
Patient 3	0.002	0.000	1.000
Patient 4	0.002	—	—
Patient 5	0.000	0.662	0.861
Patient 6	0.000	—	—
Patient 7	0.002	0.000	0.013
Patient 8	0.725	—	—

P values represent the significance of differences in the density of voxels representing the intact, regained, and nonregained visual field.

DISCUSSION

We measured properties of early visual cortex before and after vision restoration training in eight subjects with postchiasmatic lesions to the visual system. Training induced a significant visual field recovery as measured with perimetry. Our fMRI results showed that, although most voxels had no difference in receptive field location between sessions, a number of voxels had shifted their receptive field to a higher eccentricity relative to the fovea after training. In addition, BOLD responses were on average more dispersed after training, suggesting some growth of receptive field size as a result of training. However, we found no evidence for extensive representation of the regained visual field before or after training.

The changes in receptive field properties could account for small increases in visual field size as a result of training. The outward shift of receptive fields along the eccentricity axis that we observed suggests that patients learn during training to "zoom out" portions of their cortical representation. This effect was larger in the damaged hemisphere than in the intact hemisphere in patients that still had bilateral visual activation. Although the average shift in receptive field locations was very moderate (0.13° of visual angle), BOLD responses in individual voxels could show changes in lag that accounted for >1° in the visual field. Importantly, this would be an effective method for visual field enlargement in the affected hemifield only in the case of incomplete destruction of the primary visual cortex. This is supported by the notion that training is more beneficial in cases where there is functional tissue remaining in the affected hemisphere (Kasten et al. 1998a; Zihl and von Cramon 1979, 1985). Increases in receptive field size could further contribute to visual field recovery. This effect was also larger in the damaged hemisphere than that in the intact hemisphere. It has been suggested that training effects are induced by neural mechanisms for spatial attention (Chokron et al. 2008), which is backed up by fMRI data showing that training increases activity in brain areas that are associated with shifts in spatial attention (Marshall et al. 2008). It has also been suggested that these mechanisms of attention can cause structural changes with vision restoration therapy (Poggel et al. 2004). Studies in nonhuman primates have shown that attention can induce changes in the input that is driving V1 neurons. Attention in the periphery increases the summation area of individual neurons,

probably through horizontal or feedback connections, thereby effectively increasing receptive field sizes (Roberts et al. 2007). Note that the significant changes that we observed in individual subjects could theoretically be part of normal random fluctuations over time, although it is unlikely that such fluctuations would show a consistent pattern across subjects as we observed in this experiment. In addition, because patients demonstrated a stable visual field defect before training, it is unlikely that these fluctuations are a part of natural recovery.

We found no evidence for extensive representation of the impaired visual field at the level of the early visual cortex. It has been suggested that training exploits remaining functions of early visual cortex that somehow do not contribute to conscious vision (Ho et al. 2009). Such a mechanism predicts the presence of neuronal representation of the impaired parts of the visual field already before training. However, it has been shown in patients with cerebral blindness that the visual fields as measured with fMRI and those that are measured with subjective perimetry show substantial overlap (Furuta et al. 2009). This limits the possible contribution of residual capacity to vision restoration. Our fMRI results also showed a high overlap with perimetry data before training, except in some patients where the regained area that was mapped was small. However, it is likely that there are some irregularities in determining the receptive field locations of voxels—e.g., the mapping stimuli that we used were both moving in a single direction (contracting rings and a clockwise rotation wedge)—so that intervoxel differences in hemodynamic properties could cause some divergences. This can result in coupling voxels to visual field map locations that are blind according to perimetry, whereas in fact they are responding to the nonblind locations at the visual field border. Although this does not affect the estimation of the relative changes in receptive field locations between sessions, it can induce noise in coupling the fMRI to the perimetry results. This noise will have a relatively stronger effect when making comparisons with small portions of the visual field.

We also found no evidence for the emergence of a second representation in the intact hemisphere after training. Henriksson et al. (2007) reported that after training, stimulation of both the impaired hemifield and the normal hemifield resulted in brain activation in the intact hemisphere in a patient with homonymous hemianopia, as measured with both fMRI and magnetoencephalography. This would imply that neurons gained a second receptive field or that a subpopulation of neurons within a voxel shifted their receptive field to the ipsilateral hemifield. Our study did not confirm their finding because the amount of variance that could be explained by a secondary response did not increase between sessions. It should be taken into account, however, that the stimuli in our experiment were not dedicated to detect the presence of dual representations within single voxels, which may have hampered our ability to measure the type of training effect that was observed by Henriksson et al. (2007). A secondary representation, for example, would be difficult to detect with normal retinotopic mapping when it is diffusely organized. Other mapping techniques that are now available may be better suited for addressing this issue more directly (Dumoulin and Wandell 2008). Alternatively, the formation of a second receptive field may occur only after prolonged training (i.e., over 200 h in 2 yr, as in Henriksson et al. 2007), but this would also imply that the neural substrate of the field recovery would change over time.

As a whole, we found no evidence for any neural mechanism that can account for the large increases in visual field size that are observed in some patients with complete hemianopias (Mueller et al. 2007). Considering the cortical magnification factor, representation of the restored visual field in early visual cortex would require large-scale neuronal reorganization. The two patients in our study that demonstrated such an increase in visual field size had no signs of neuronal representation of the damaged visual field before or after training. Because these increases in visual field size were measured with extensive eye movement control, we believe it is highly unlikely that the findings in these two subjects are confounded (Bergsma and Van der Wildt 2010). This suggests that training somehow helps these patients to use visual information that enters the brain through alternative neuronal pathways. For example, it has been shown that the middle temporal area (MT) still produces visually evoked responses after removal of V1 (Rodman et al. 1989), which could be related to connectivity between the lateral geniculate nucleus (LGN) and MT (Sincich et al. 2004). There is also recent evidence obtained with diffusion tensor imaging that the connectivity between the LGN and MT changes after destruction of the primary visual cortex (Bridge et al. 2008). Also, connections between the retina and the superior colliculus could play a role (Cowey and Stoerig 1991). Such alternative connectivity could explain that training locations deep within the absolute blind field can still have beneficial effects for hemianopic patients (Jobke et al. 2009). It is unclear, however, whether visual representation that is established through alternative routes, without parallel representation in the primary visual cortices, results in vision that is qualitatively comparable with normal vision. These alternative routes lack most of the common mechanisms for feature detection that are present in early visual cortices. Imaging data even suggest that they might not even induce conscious visual experiences (Goebel et al. 2001). On the other hand, they could be important for guiding behavioral compensation, such as making eye or head movement toward visual events or evading objects during locomotion.

In this study we continuously measured eye movements during perimetry and carefully monitored eye movements during the training sessions, but did not record eye movements during the functional mapping experiments in the scanner. We did not use an attentional task at central fixation since that could interfere with the training effects because the training effects may be the result of changes in attentional control by the patients; however, it is highly unlikely that our results in the scanner are caused by stable eccentric fixation or unstable fixation. In the case of stable eccentric fixation, a shift of receptive field locations in one hemifield would be accompanied with a shift in the same direction in the other hemifield. If patients would have shifted their gaze toward the lesion, for example, then the receptive field locations of voxels would have shifted toward the opposite direction across the entire visual field. The outward shift in receptive field locations that we observed produced opposite shifts in the two hemifields. The influence of fixation instability on responses during retinotopic mapping, however, is more complex and less predictable. In any event, it would disturb the regular cyclic responses during mapping stimuli, thereby producing on average lower

and more dispersed BOLD responses. Although we observed reduced amplitudes and increased dispersion of BOLD responses after training in some patients, these reductions did not correlate with the shift of receptive field locations toward the eccentricity. We therefore believe it is unlikely that the shift in receptive field locations can be explained by more random eye movements after training. Furthermore, the observed (nonsignificant) correlation between changes in response amplitude and dispersion was positive and thus the reverse of what would be expected when both are caused by fixation instability. The pattern of results as a whole does not suggest that eye movements play a role in the current findings. It should also be taken into account that reductions in amplitudes of BOLD responses are not necessarily caused by eye movements; for example, lower BOLD responses have been linked to decreases in effort as a result of learning as well (Jansma et al. 2001). On the other hand, signal reductions during retesting have also been observed with fMRI without extensive training between sessions (Clement and Belleville 2009; Raemaekers et al. 2007; Zandbelt et al. 2008). These reductions may be related to the novelty of the mapping stimuli or the scanner environment when subjects are in the MRI scanner for the first session. Our study did not include a control group and, to our knowledge, no studies have addressed the test–retest reliability of BOLD responses during retinotopic mapping, so no definite conclusions can be drawn regarding this matter.

In conclusion, we have found changes in receptive field locations and sizes that could return vision to a small portion of the visual field in patients with cerebral blindness. Although large increases in visual field were observed in some patients, we did not observe changes in early visual cortex that could account for them.

DISCLOSURES

No conflicts of interest, financial or otherwise, are declared by the authors.

REFERENCES

Ashburner J, Friston KJ. Unified segmentation. *NeuroImage* 26: 839–851, 2005.

Bergsma DP, Van der Wildt GJ. Properties of the regained visual field after visual detection training of hemianopsia patients. *Restor Neurol Neurosci* 26: 365–375, 2008.

Bergsma DP, Van der Wildt GJ. Visual training of cerebral blindness patients gradually enlarges the visual field. *Br J Ophthalmol* 94: 88–96, 2010.

Bridge H, Thomas O, Jbabdi S, Cowey A. Changes in connectivity after visual cortical brain damage underlie altered visual function. *Brain* 131: 1433–1444, 2008.

Chokron S, Perez C, Obadia M, Gaudry I, Laloum L, Gout O. From blindsight to sight: cognitive rehabilitation of visual field defects. *Restor Neurol Neurosci* 26: 305–320, 2008.

Clement F, Belleville S. Test–retest reliability of fMRI verbal episodic memory paradigms in healthy older adults and in persons with mild cognitive impairment. *Hum Brain Mapp* 30: 4033–4047, 2009.

Cowey A, Stoerig P. The neurobiology of blindsight. *Trends Neurosci* 14: 140–145, 1991.

Dumoulin SO, Wandell BA. Population receptive field estimates in human visual cortex. *NeuroImage* 39: 647–660, 2008.

Furuta A, Nakadomari S, Misaki M, Miyauchi S, Iida T. Objective perimetry using functional magnetic resonance imaging in patients with visual field loss. *Exp Neurol* 217: 401–406, 2009.

Goebel R, Muckli L, Zanella FE, Singer W, Stoerig P. Sustained extrastriate cortical activation without visual awareness revealed by fMRI studies of hemianopic patients. *Vision Res* 41: 1459–1474, 2001.

Golay X, Pruessmann KP, Weiger M, Crelier GR, Folkers PJ, Kollias SS, Boesiger P. PRESTO-SENSE: an ultrafast whole-brain fMRI technique. *Magn Reson Med* 43: 779–786, 2000.

Henriksson L, Raninen A, Nasanen R, Hyvarinen L, Vanni S. Training-induced cortical representation of a hemianopic hemifield. *J Neurol Neurosurg Psychiatry* 78: 74–81, 2007.

Ho YC, Cheze A, Sitoh YY, Petersen ET, Goh KY, Gjedde A, Golay X. Residual neurovascular function and retinotopy in a case of hemianopia. *Ann Acad Med Singapore* 38: 827–831, 2009.

Jansma JM, Ramsey NF, Slagter HA, Kahn RS. Functional anatomical correlates of controlled and automatic processing. *J Cogn Neurosci* 13: 730–743, 2001.

Jobke S, Kasten E, Sabel BA. Vision restoration through extrastriate stimulation in patients with visual field defects: a double-blind and randomized experimental study. *Neurorehabil Neural Repair* 23: 246–255, 2009.

Julkunen L, Tenovuo O, Jaaskelainen S, Hamalainen H. Rehabilitation of chronic post-stroke visual field defect with computer-assisted training: a clinical and neurophysiological study. *Restor Neurol Neurosci* 21: 19–28, 2003.

Kasten E, Bunzenthal U, Sabel BA. Visual field recovery after vision restoration therapy (VRT) is independent of eye movements: an eye tracker study. *Behav Brain Res* 175: 18–26, 2006.

Kasten E, Poggel DA, Sabel BA. Computer-based training of stimulus detection improves color and simple pattern recognition in the defective field of hemianopic subjects. *J Cogn Neurosci* 12: 1001–1012, 2000.

Kasten E, Wüst S, Sabel BA. Residual vision in transition zones in patients with cerebral blindness. *J Clin Exp Neuropsychol* 20: 581–598, 1998a.

Kasten E, Wüst S, Behrens-Baumann W, Sabel BA. Computer-based training for the treatment of partial blindness. *Nat Med* 4: 1083–1087, 1998b.

Marshall RS, Ferrera JJ, Barnes A, Xian Z, O'Brien KA, Chmayssani M, Hirsch J, Lazar RM. Brain activity associated with stimulation therapy of the visual borderzone in hemianopic stroke patients. *Neurorehabil Neural Repair* 22: 136–144, 2008.

Mueller I, Mast H, Sabel BA. Recovery of visual field defects: a large clinical observational study using vision restoration therapy. *Restor Neurol Neurosci* 25: 563–572, 2007.

Neggers SF, Hermans EJ, Ramsey NF. Enhanced sensitivity with fast three-dimensional blood-oxygen-level-dependent functional MRI: comparison of SENSE-PRESTO and 2D-EPI at 3 T. *NMR Biomed* 21: 663–676, 2008.

Poggel DA, Kasten E, Muller-Oehring EM, Sabel BA, Brandt SA. Unusual spontaneous and training induced visual field recovery in a patient with a gunshot lesion. *J Neurol Neurosurg Psychiatry* 70: 236–239, 2001.

Poggel DA, Kasten E, Sabel BA. Attentional cueing improves vision restoration therapy in patients with visual field defects. *Neurology* 63: 2069–2076, 2004.

Raemaekers M, Vink M, Zandbelt B, van Wezel RJ, Kahn RS, Ramsey NF. Test–retest reliability of fMRI activation during prosaccades and antisaccades. *NeuroImage* 36: 532–542, 2007.

Reinhard J, Schreiber A, Schiefer U, Kasten E, Sabel BA, Kenkel S, Vonthein R, Trauzettel-Klosinski S. Does visual restitution training change absolute homonymous visual field defects? A fundus controlled study. *Br J Ophthalmol* 89: 30–35, 2005.

Roberts M, Delicato LS, Herrero J, Gieselmann MA, Thiele A. Attention alters spatial integration in macaque V1 in an eccentricity-dependent manner. *Nat Neurosci* 10: 1483–1491, 2007.

Rodman HR, Gross CG, Albright TD. Afferent basis of visual response properties in area MT of the macaque. I. Effects of striate cortex removal. *J Neurosci* 9: 2033–2050, 1989.

Sahraie A. Induced visual sensitivity changes in chronic hemianopia. *Curr Opin Neurol* 20: 661–666, 2007.

Schmielau F, Wong EK Jr. Recovery of visual fields in brain-lesioned patients by reaction perimetry treatment (Abstract). *J Neuroeng Rehabil* 4: 31, 2007.

Schumacher EH, Jacko JA, Primo SA, Main KL, Moloney KP, Kinzel EN, Ginn J. Reorganization of visual processing is related to eccentric viewing in patients with macular degeneration. *Restor Neurol Neurosci* 26: 391–402, 2008.

Sincich LC, Park KF, Wohlgemuth MJ, Horton JC. Bypassing V1: a direct geniculate input to area MT. *Nat Neurosci* 7: 1123–1128, 2004.

Van der Wildt GJ, Bergsma DP. Visual field enlargement by neuropsychological training of a hemianopsia patient. *Doc Ophthalmol* 93: 277–292, 1997.

Van Essen DC, Drury HA, Dickson J, Harwell J, Hanlon D, Anderson CH. An integrated software suite for surface-based analyses of cerebral cortex. *J Am Med Inform Assoc* 8: 443–459, 2001.

Zandbelt BB, Gladwin TE, Raemaekers M, van Buuren M, Neggers SF, Kahn RS, Ramsey NF, Vink M. Within-subject variation in BOLD-fMRI signal changes across repeated measurements: quantification and implications for sample size. *NeuroImage* 42: 196–206, 2008.

Zhang X, Kedar S, Lynn MJ, Newman NJ, Biousse V. Natural history of homonymous hemianopia. *Neurology* 66: 901–905, 2006.

Zihl J, von Cramon D. Restitution of visual function in patients with cerebral blindness. *J Neurol Neurosurg Psychiatry* 42: 312–322, 1979.

Zihl J, von Cramon D. Visual field recovery from scotoma in patients with postgeniculate damage. A review of 55 cases. *Brain* 108: 335–365, 1985.